

RSC Advances



This is an *Accepted Manuscript*, which has been through the Royal Society of Chemistry peer review process and has been accepted for publication.

Accepted Manuscripts are published online shortly after acceptance, before technical editing, formatting and proof reading. Using this free service, authors can make their results available to the community, in citable form, before we publish the edited article. This *Accepted Manuscript* will be replaced by the edited, formatted and paginated article as soon as this is available.

You can find more information about *Accepted Manuscripts* in the [Information for Authors](#).

Please note that technical editing may introduce minor changes to the text and/or graphics, which may alter content. The journal's standard [Terms & Conditions](#) and the [Ethical guidelines](#) still apply. In no event shall the Royal Society of Chemistry be held responsible for any errors or omissions in this *Accepted Manuscript* or any consequences arising from the use of any information it contains.

Cite this: DOI: 10.1039/c0xx00000x

www.rsc.org/xxxxxx

ARTICLE TYPE

Room-temperature synthetic NiFe layered double hydroxide with different anions intercalation as an excellent oxygen evolution catalyst

Yuqi Xu ‡^a, Yongchao Hao ‡^a, Guoxin Zhang^a, Zhiyi Lu^a, Shuang Han^a, Yaping Li*^a, Xiaoming Sun*^a

Received (in XXX, XXX) Xth XXXXXXXXX 20XX, Accepted Xth XXXXXXXXX 20XX

DOI: 10.1039/b000000x

Ni-Fe layered double hydroxide (LDH) was regarded one of the best catalysts for oxygen evolution reaction (OER), yet bridging the relationship between LDH nanostructure and OER performance remains a big challenge. Unlike other hydrothermal reaction produced Ni-Fe layered double hydroxides, we adopted a simple separate nucleation and the aged steps method to investigate the effect of crystallinity and intercalated anions of LDH on OER performance and found that improving the crystallinity and the size of NiFe-LDH by increasing the aged temperature led to the decrease of OER activity. While changing the interlayer spacing of LDH from 8.04 Å to 7.69 Å through introducing more CO₃²⁻ to replace NO₃⁻ causes the reduction of OER activity. These were probably attributed to more exposed active sites, lower charger transferring resistance, and better exchange ability with OH⁻ in interlamination. Based on above observation and the consequent optimizations, a very-low onset overpotential (~240 mV) and Tafel slope value (33.6 mV/dec) (in 0.1 mol/L KOH) room-temperature synthetic NiFe LDH was achieved. This work proposed the strategy for the rational design of LDHs for further enhancement of OER electrochemical activity, i.e. by decreasing the size and crystallinity of NiFe-LDH and introducing more NO₃⁻ between layers.

1. Introduction

The high-efficiency, eco-friendly, low-cost energy storage applications is a critical element in the societal pursuit of sustainable and efficient energy conversion and storage solutions. The oxygen evolution reaction (OER) in particular is a key factor of many renewable energy systems, such as metal-air battery and water splitting.²⁻³ Thus, it is important to develop cost-effective, highly active catalysts for OER. Precious noble-metal oxides catalysts such as IrO₂ and RuO₂ show considerable catalytic activity for OER but they suffer from the scarcity and high cost.³⁻⁵ As a consequence, extensive efforts have been taken to discover and develop efficient OER catalysts based on earth-abundant metals, especially the nickel-based catalysts.⁵⁻¹⁰

Layered double hydroxides (LDHs), which are a kind of anion-intercalated materials, have newly drawn great attention in the OER area due to their uniformly and densely distributed active sites.¹⁰⁻¹⁴ Meanwhile, the abundance of constituent elements, the easiness of fabrication, the capability of highly tunable compositions, and the superior OER performance made them to be rising stars, giving the possibility of practical utilization for electrochemically splitting water and any applications involved OER such as metal-air batteries.¹⁴⁻¹⁵ Among these LDHs catalysts, NiFe-LDH was the most studied in recent years.¹³⁻¹⁸ As the three important factors which have strong effect on properties of LDH, when the metal elements are determined, the other two aspects may give great impact on the

OER performance under given NiFe-LDH: one is the size and crystallinity of catalysts, the other is the intercalated anions between LDH's layers.¹⁹

In order to validate our assumptions, we finely tuned the crystallinity and sheet size by varying the aged temperature and altered the intercalation anions. It was noticed that the higher aged temperature applied, the higher crystallinity the LDH will be and consequently, the more the active sites will be confined, as verified by OER data. Interlayer spacing was tuned by varying the ratio of OH⁻ with CO₃²⁻ from 24:0 to 24:2 and 24:4, while NO₃⁻ were used as the intercalated ions. More CO₃²⁻ would cause 4% decrease of the interlayer spacing, which gave a trend of interlayer shrinking. Despite the small difference in interlayer spacing, we observed obvious OER current variance at the same applied voltages. Based on the above results, we safely hypothesized the most active and efficient OER catalysts that were base on LDH could be generated on conditions of small size, low crystallinity, and more intercalated NO₃⁻.

2. Experimental

2.1. Chemicals

Ni(NO₃)₂·6H₂O and Fe(NO₃)₃·6H₂O was obtained from Xilong Chemical Co., Ltd., and Tianjin Fu Chen Chemical Reagents, respectively. NaOH and Na₂CO₃ were all of A.R. grade, and purchased from Beijing Chemical Reagent Co., Ltd., and used as received without further purification. Deionized water has been bubbled with N₂ for 1 h to remove CO₂.

2.2. Synthesis of NiFe-LDH

In a typical procedure, 10.0 mL of mixed salt solution containing $\text{Ni}(\text{NO}_3)_2 \cdot 6\text{H}_2\text{O}$ (2.4 mmol) and $\text{Fe}(\text{NO}_3)_3 \cdot 6\text{H}_2\text{O}$ (0.8 mmol) and 40.0 mL of mixed alkali solution containing NaOH and Na_2CO_3 ($n_{\text{NaOH}} + 2n_{\text{Na}_2\text{CO}_3} = 7.2$ mmol, $n_{\text{NaOH}}:n_{\text{Na}_2\text{CO}_3} = 24:0, 24:2, \text{ or } 24:4$) were simultaneously poured out into a colloidal mill and continuously stirred for 10 min. The resulted slurry was centrifuged at 12,000 rpm for 15 min and washed twice with deionized water to remove the excess free metal salts and alkali, and subsequently dispersed in 40.0 mL of deionized water. This aqueous suspension was transferred into a stainless steel autoclave with a teflon lining. The autoclave was then placed in a preheated oven, followed by hydrothermal treatment at room temperature (RT), 90, 120 and 150 °C for 12 h. The products were collected by centrifuge, repetitively washed with CO_2 -free deionized water and lyophilized.

2.3. Characterization

Transmission electron microscopy (TEM) was performed on Hitachi-800 (accelerating voltage = 200 kV). X-ray diffraction (XRD) patterns were obtained on a Shimadzu XRD-6000 diffractometer, using $\text{Cu K}\alpha$ radiation ($\lambda = 1.5418 \text{ \AA}$) at 40 kV, 30 mA. Fourier transform infrared (FT-IR) spectra were recorded in the range 4000 to 400 cm^{-1} with 2 cm^{-1} resolution on a Bruker Vector-22 fourier transform spectrometer using the KBr pellet technique (1 mg of sample in 100 mg of KBr). XPS measurements were performed using an ESCALAB 250 instrument (Thermo Electron) with Al KR radiation. The CHN analysis was executed with a varioELcube elemental analyzer.

2.4. Electrochemical measurements

All electrochemical measurements were performed on standard three-electrode setup at RT. Electrochemical measurements (using a PARSTAT 2273 potentiostat from Princeton Applied Research) were conducted in an electrochemical cell using saturated calomel electrode (SCE, 1.01 V vs. RHE in 0.1 M KOH) as the reference electrode, a 1- cm^2 Pt plate as the counter electrode and the sample modified glassy carbon electrode (GCE) as the working electrode. For the rotating disk electrode (RDE) measurements, the working electrode was scanned cathodically at a rate of 5 mV s^{-1} with a speed of 1600 rpm. Linear sweep voltammetry (LSV) was carried out at 5 mV/s for the polarization curves after the catalyst was cycled for 10 times by cyclic voltammetry (CV) in the oxygen saturated 0.1 M KOH aqueous solutions at a sweep rate of 50 mV s^{-1} from 0.2 to 0.7 V, respectively. Prior to surface coating, the GCE was sequentially polished using 1.0 and 0.3 mm alumina slurry and then washed ultrasonically in water and ethanol for 5 min. The cleaned GCE was dried at RT for the next modification.

For RDE measurements, 2.0 mg catalyst was dispersed in 490.0 μL of ethanol and 10.0 μL of 5% nafion solution and sonicated for 30 min to form a homogeneous ink. Then 5.0 μL of the catalyst ink was loaded onto the cleaned GCE (5 mm in diameter, area of 0.196 cm^2). The All polarization curves were corrected with iR-compensation.

3. Results and discussion

The targeted NiFe-LDHs were prepared according to the

separate nucleation and the aged steps (SNAS) method in which the salt and the alkali solutions were quickly mixed and nucleated in a colloid mill and subsequent hydrothermally treated.²⁰⁻²¹ Fig 1 and Fig S1, the typical TEM images, revealed that NiFe-LDHs displayed plate-like morphology with growing size from RT to 150 °C (Fig 1f). The corresponding XRD spectra (Fig 1e, Fig S2a-b) showed that the (003) and the (006) peaks were significantly broadened and weakened with depressed aging temperature, suggesting the less crystallinity and more defects in the stacked structure.²²⁻²⁸ The lateral sizes of NiFe-LDH nanosheets with no CO_3^{2-} was 16, 33, 61, and 143 nm in average for RT, 90, 120 and 150 °C-aged samples, respectively (Fig. 1f). And the typical size is labelled in TEM image to highlight the difference (Fig. 1a-d). The other different anions-intercalated NiFe-LDHs also showed similar size growth at the same aging temperature (Fig. S1).

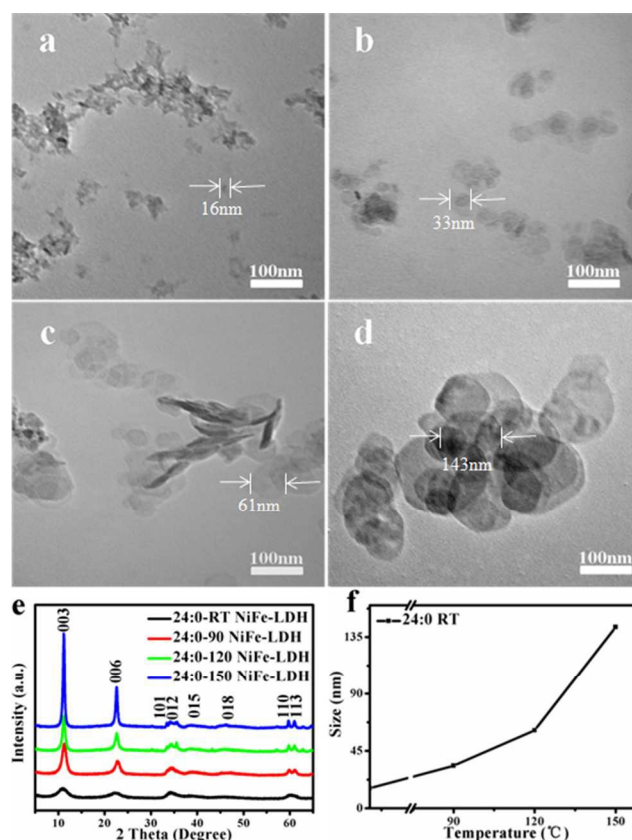


Fig 1. TEM images of NiFe-LDH plates under different resultant temperature for 12 h with a 24:0 ratio of NaOH and Na_2CO_3 : (a) RT, (b) 90 °C, (c) 120 °C, (d) 150 °C and (e) their XRD spectra, (f) size distribution.

To demonstrate the difference of intercalated anions (NO_3^- or CO_3^{2-}), Fourier transformed infrared spectra of the RT-aged samples were collected and shown in Fig.2a, which was recorded in the range from 2000 to 1000 cm^{-1} . The infrared band at 1631 cm^{-1} is attributed to the deformation mode of water ($\delta(\text{H}_2\text{O})$) while the band at 1384 cm^{-1} stands for NO_3^- .^{21, 24} As the CO_3^{2-} increased, two new broad bands at about 1470 cm^{-1} , and the one between 1000 and 1200 cm^{-1} occurred, which were assigned to the CO_3^{2-} . Meanwhile, a typical vibration of interlayer CO_3^{2-} -band

at 1357 cm^{-1} appeared and grew strong; besides, the ν_3 (asymmetric stretching) mode of NO_3^- at 1384 cm^{-1} band which turned weak, suggesting that NO_3^- had been exchanged by CO_3^{2-} .²⁶⁻²⁷ In addition, the other important mode $\nu(\text{OH}^-)$, $\delta(\text{OH}^-)$ and ν_1 (CO_3^{2-}) were labeled in Fig. S4. Besides, with a varioELcube elemental analyzer, we found that the nitrogen content of NiFe-LDH with 24:0-RT, 24:2-RT, 24:4-RT was 0.676%, 0.413% and 0.22% in weight respectively, which is agreed with FT-IR results. As shown in Fig. 2b, with the more NO_3^- exchanged by CO_3^{2-} in the synthesis step (24:0 to 24:4), the (003) Bragg reflection gradually shifted from 8.04 \AA to 7.82 \AA then 7.69 \AA . And for the complete NO_3^- batch, the interlayer spacing is the same to that of NO_3^- intercalated MgFe-LDH (8.04 \AA) prepared by the coprecipitation.²⁷

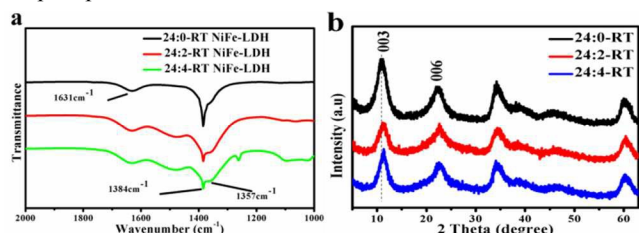


Fig 2. (a) The FT-IR and XRD spectra (b) of NiFe-LDH OER catalyst with various ratios of NaOH and Na_2CO_3 at RT.

The products with the lowest applied aged temperature, *i.e.* RT yielded the best electrocatalytic activity in 0.1 M KOH aqueous solution (Fig 3a, Fig. S3a-b). It is in accord with the fact that the defects are generally active sites for water splitting reactions.³⁰⁻³² Especially, those RT-catalysts exhibit superior OER activity to commercial Ir/C in alkaline medium. Under high aged temperature, consequently elevated crystallinity and depressed disorder (Fig.1e, Fig S2), the sheet size grew bigger (Fig.1f) and those defects concentration decreased, which provided less activity towards OER reactions. This was consistent with the report that the amorphous phase showed the superior OER activity to the crystalline ones.³⁰

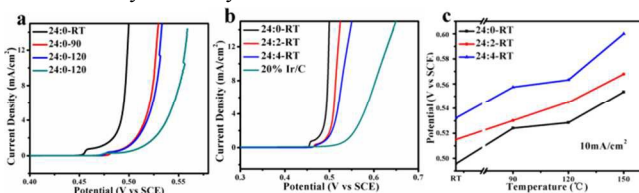


Fig 3. (a) The electrochemical performance of NiFe-LDH aged under different resultant temperature with a 24:0 ratio of NaOH and Na_2CO_3 . (b) The OER activity of NiFe-LDH with different ratios of NaOH and Na_2CO_3 at RT. (c) The potentials at 10 mA/cm^2 current for all samples. The loading of all samples was about 0.1 mg/cm^2 .

Besides the aged temperature, we found the ratios of different anion intercalated being another vital parameter to enhance OER performance (Fig 3b-c). Given the difference ratio of intercalated anions, the interlayer spacing could be affected. XRD characterizations were performed to verify varied interlayer spacing of resulted LDHs. It was found that larger interlayer distance induced by less CO_3^{2-} was relative to smaller overpotential for OER, which means higher activity. However,

considering the small change of the interlayer spacing, we safely believed that the intercalated anions play more important roles in OER catalytic process instead of lamellar spacing of LDHs.¹⁹

In order to illustrate the intercalated anions and interlayer spacing being the important factors which affect overall OER performance for the RT aged temperature NiFe-LDHs, XPS analysis of samples synthesized at RT but with different ratios of OH^- and CO_3^{2-} were performed. The Ni2p and Fe2p XPS spectra were respectively shown in the Fig. S5a-b. The oxidation states of Ni and Fe were found to be Ni^{2+} and Fe^{3+} ; the ratios of Ni and Fe kept almost the same with each other for the three samples.¹³ Given the situation that no obvious binding energy (BE) shift occurred, we can safely conclude that chemical states remain the same within these three samples obtained at RT.

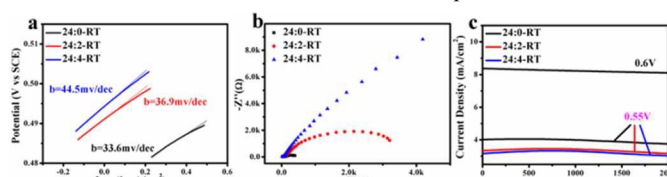


Fig. 4 The current–time plots (a) of the different NiFe-LDH electrodes under the same alkaline conditions with various ratios of NaOH and Na_2CO_3 under RT and corresponding Tafel plots (b), Nyquist plots (c) with a frequency range from 0.1 MHz to 1 Hz.

Tafel slopes were then measured to investigate the electrode kinetics. As shown in Fig 4a, the corresponding Tafel slope values were respectively 33.6, 36.9, and 44.5 mV/dec, meaning total NO_3^- intercalated NiFe-LDH was more efficient OER electrocatalyst among these three samples. EIS plots (Fig. 4b) in the high frequency range indicated the intercalation by NO_3^- , and also agreed broader interlayer space possess lower charger transferring resistance (R_{ct}) at the corresponding electrode/electrolyte interface, resulting in a more favorable OER kinetics.^{9, 15, 30} The chronoamperometric tests of NiFe-LDHs were performed at 0.55 V (vs SCE, without iR correction) on the GCE. As seen in Fig 4c, NiFe-LDHs without CO_3^{2-} showed the best stability in both low and high voltages, 2,000 s cycling caused only 4.8% activity decade at 0.55 V and 3% at 0.6 V. While for the other two samples synthesized at RT, the activity 80 decades were 5.5% for 24:2 NiFe-LDH and 5% for 24:4 NiFe-LDH, respectively. Yet their current densities were relatively low compared to that of 24:0 NiFe-LDH at the same applied voltage of 0.55 V.

As a kind of anion-intercalated material, LDHs possess powerful ion exchange ability.^{16, 19, 33} And the accessibility to OH^- plays very important role in OER because OH^- is the main reactant in alkaline solution.^{1, 13} Considering that NO_3^- is easier to be exchanged by OH^- than the CO_3^{2-} , it obviously the complete NO_3^- intercalated NiFe-LDH can gather more OH^- .³³ Therefore, the reason why the sample with only NO_3^- intercalated showed the best electrocatalytic activity is because of the lowest charger transferring resistance as well as the good anion-exchange ability with hydroxyl anion.

4. Conclusions

Size, crystallinity, and intercalated anions were all found to be important in determining the activity of OER. The samples with low crystallinity were achieved through lowering the aged temperature. The variations of intercalated ions can be obtained using different amount anions of NO₃⁻ and CO₃²⁻ in the synthesis procedures. Investigations of size, crystallinity and interlayer anions on OER demonstrated that efficient OER favored small size, low crystallinity which provided more unconfined active sites. More intercalated NO₃⁻ and wider interlayer space could reduce the charger transferring resistance and improve the exchange ability with OH⁻. Our comprehensive understanding of LDH catalyzed OER process could be extended for synthesizing better layered materials for OER.

Acknowledgements

This work was financially supported by National Natural Science Foundation of China, the 973 Program (2011CBA00503 and 2011CB932403), the Fundamental Research Funds for the Central Universities, and the Program for Changjiang Scholars and Innovative Research Team in University.

Notes and references

^a State Key Laboratory of Chemical Resource Engineering, Beijing University of Chemical Technology, Beijing 100029, China.

Tel.: +8610-64438991

* Corresponding E-mail: sunxm@mail.buct.edu.cn; liyp@mail.buct.edu.cn

‡ Contributed equally to this work

† Electronic Supplementary Information (ESI) available: TEM images, XRD spectra, electrochemical characterization, Ni 2p XPS survey spectra and Fe 2p XPS survey spectra of samples and a table about OER activities of some benchmark catalysts in alkaline solution at 10 mA/cm². See DOI: 10.1039/b000000x/

[1] J. Suntivich, K. J. May, H. A. Gasteiger, H. A. Gasteiger, J. B. Goodenough, S. H. Yang, *Science* 334 (2011) 1383-1385.

[2] Y. Zhao, R. Nakamura, K. Kamiya, S. Nakanishi, K. Hashimoto, *Nat. Comm.* 4 (2013) 2390.

[3] T. Grewe, X. Deng, C. Weidenthaler, F. Schüth, H. Tüysüz, *Chem. Mater.* 25 (2013) 4926-4935.

[4] Z. Peng, D. S. Jia, A. M. Al-Enizi, A. A. Elzatahry, and G. F. Zheng, *Adv. Energy Mater.* 5 (2015) 1402031

[4] L. Trotochaud, J. K. Ranney, K. N. Williams, S. W. Boettcher, *J. Am. Chem. Soc.* 134 (2014) 17253-17261.

[5] M. Zhang, M. T. Zhang, C. Hou, Z. F. Ke, T. B. Lu, *Angew. Chem. Int. Ed.* 53 (2014) 13042-13048.

[6] M. J. Kenney, M. Gong, Y. Li, J. Z. Wu, J. Feng, M. Lanza, H. Dai, *Science* 342 (2013) 836-840.

[7] M. W. Louie, A. T. Bell, *J. Am. Chem. Soc.* 135 (2013) 12329-12337.

[8] W. Zhou, X. J. Wu, X. Cao, X. Huang, C. Tan, J. Tian, H. Liu, J. Wang, H. Zhang, *Energy Environ. Sci.* 6 (2013) 2921-2924.

[9] S. Chen, J. Duan, M. Jaroniec, S. Z. Qiao, *Angew. Chem. Int. Ed.* 52 (2013) 13567-13570.

[10] Z. Lu, W. Xu, W. Zhu, Q. Yang, X. Lei, J. Liu, Y. Li, X. Sun, X. Duan, *Chem. Commun.* 50 (2014) 6479-6482.

[11] C. G. Silva, Y. Bouzidi, V. Fornés, H. Garcia, *J. Am. Chem. Soc.* 131 (2009) 13833-13839.

[12] Y. Zhao, B. Li, Q. Wang, W. Gao, C. J. Wang, M. Wei, D. G. Evans, X. Duan, D. O'Hare, *Chem. Sci.* 5 (2014) 951-958.

[13] M. Gong, Y. Li, H. Wang, Y. Liang, J. Z. Wu, J. Zhou, J. Wang, T. Regier, F. Wei, H. Dai, *J. Am. Chem. Soc.* 135 (2013) 8452-8455.

[14] J. Jiang, A. L. Zhang, L. L. Li, L. H. Ai, *J. Power Sources*, 2015, 278: 445-451.

[15] X. Long, J. Li, S. Xiao, K. Yan, Z. Wang, H. Chen, S. Yang, *Angew. Chem.* 126 (2014) 7714-7718.

[16] F. Song, X. Hu, *Nat. Comm.* 5 (2014) 4477.

[17] B. M. Hunter, J. D. Blakemore, M. Deimund, H. B. Gray, J. R.

Winkler, A. M. Müller, *J. Am. Chem. Soc.* 136 (2014) 13118-13121.

[18] D. Tang, J. Liu, X. Wu, R. Liu, X. Han, Y. Han, H. Huang, Y. Liu, Z. Kang, *ACS Appl. Mater. Interfaces* 6 (2014) 7918-7925.

[19] Q. Wang and D. O'Hare, *Chem. Rev.* 112(2012): 4124-4155.

[20] Z. Chang, C. Wu, S. Song, Y. Kuang, X. Lei, L. Wang, X. Sun, *Inorg. Chem.* 52 (2013) 8694-8698.

[21] Q. Zhang, J. Xu, D. Yan, S. Li, J. Lu, X. Cao, B. Wang, *Catal. Sci. Technol.* 3 (2013) 2016-2024.

[22] L. Li, R. Ma, Y. Ebina, K. Fukuda, K. Takada, T. Sasaki, *J. Am. Chem. Soc.* 129 (2007) 8000-8007.

[23] N. T. Whilton, P. J. Vickers, S. Mann, *J. Mater. Chem.* 7 (1997) 1623-1629.

[24] F. Millange, R. I. Walton, D. O'Hare, *J. Mater. Chem.* 10 (2000) 1713-1720.

[25] C. Tavio-Guého, Y. Feng, A. Faour, F. Leroux, *Dalton Trans.* 39 (2010) 5994-6005.

[26] Y. Lee, J. H. Choi, H. J. Jeon, K. M. Choi, J. W. Lee, J. K. Kang, *Energy Environ. Sci.* 4 (2011) 914-920.

[27] F. Z. Zhang, L. L. Zhao, H. Y. Chen, S. L. Xu, D. G. Evans, and X. Duan, *Angew. Chem. Int. Ed.* 2008, 47, 2466-2469.

[28] Z. P. Liu, R. Z. Ma, M. Osada, N. Iyi, Y. Ebina, K. Takada, and T. Sasaki, *J. Am. Chem. Soc.*, 2006, 128, 4872-4880.

[29] R. Ma, Z. Liu, K. Takada, N. Iyi, Y. Bando, T. Sasaki, *J. Am. Chem. Soc.* 129 (2007) 5257-5263.

[30] R. D. L. Smith, M. S. Prévot, R. D. Fagan, Z. Zhang, P. A. Sedach, M. K. J. Siu, S. Trudel, C. P. Berlinguette, *Science* 340 (2013) 60-63.

[31] A. Bergmann, I. Zaharieva, H. Dau, Peter Strasser, *Energy Environ. Sci.*, 2013, 6, 2745-2755.

[32] F. Y. Cheng, J. Shen, B. Peng, Y. D Pan, Z. L. Zhan, J. Chen. *Nat. Chem.*, 2011, 3(1): 79-84.

[33] S. Miyata, *Clays Clay Miner* 31 (1983) 305-311.